*Pol. J. Environ. Stud. Vol. XX, No. X (XXXX), 1-12*
DOI: *10.15244/pjoes/235729* ONLINE PUBLICATION DATE: 2026-11-03

*Original Research*

# Spatial Distribution and Source Apportionment of Nitrate in Groundwater in a Representative Agricultural Region of the Southern Piedmont of the Qinling Mountains, China

**Hao Zhao[1, 2], Wenqiang Gong[1, 2]*, Jianwei Sun[1, 2]**, Xinbin Li[1, 2], Xianda Cheng[1, 2], Chao Zhao[1, 2], Haiyang Yue[1], Chaohui Han[1, 2]**

[1]Xi'an Mineral Resources Survey, China Geological Survey, Xi'an 710100, China
[2]Qinling-Loess Plateau Transition Zone Observation and Research Station for Coupling of Soil and Water Elements and Conservation of Biological Resources, Tongguan 714300, China

*Received: 09 March 2026*
*Accepted: 27 August 2026*

## Abstract

As a critical ecological barrier and core water conservation zone in China, the southern slope of the Qinling Mountains plays a pivotal role in safeguarding regional ecological security and ensuring a safe drinking water supply, largely mediated by groundwater quality. However, systematic investigations into nitrate contamination in this region remain limited, and the dominant sources as well as hydrogeochemical migration pathways of nitrate are still poorly constrained. To address these knowledge gaps, this study targets representative watersheds on the southern slope of the Qinling Mountains, with an emphasis on characterizing the spatial – temporal distribution patterns and identifying the primary sources of groundwater nitrate. A multi-gradient monitoring network was established along the Han River and its tributaries, supporting seasonal sampling across both dry and wet periods. Coupled with $\delta^{15}N$-$\delta^{18}O$ dual-isotope tracing and comprehensive regional environmental background surveys, we quantitatively assessed the spatial heterogeneity, temporal dynamics, and source apportionment of nitrate in groundwater. Results reveal pronounced spatial variability: mean nitrate concentrations decrease downstream, and levels adjacent to the main stem are consistently lower than those in tributary zones. Furthermore, the spatial distribution of nitrate closely parallels the regional groundwater flow direction. Vertically, soil nitrate concentrations decline with depth overall, yet exhibit anomalous enrichment at a depth of ~1 m – indicating that nitrate leaching has penetrated to at least this depth. Source apportionment indicates that soil nitrogen, livestock and poultry manure, and domestic sewage collectively account for the majority of nitrate inputs to groundwater. This study provides foundational observational data on groundwater nitrogen cycling in mountain – basin transitional zones, thereby strengthening the scientific basis for groundwater protection and ecosystem management in the region.

*e-mail: gongwenqiang2024@163.com
Tel.: +0086-166-029-048-89
**e-mail: sun-jianwei@163.com
Tel.: +0086-189-356-882-20
0009-0000-1309-3611

© 2026 This article is licensed under a Creative Commons Attribution-NonCommercial 4.0 International (CC BY-NC 4.0)

It also advances theoretical understanding of nitrogen biogeochemistry in complex terrain and supports the development of targeted, evidence-based groundwater pollution mitigation strategies.

**Keywords:** groundwater, sources of nitrate, nitrogen and oxygen isotopes, Qinling Mountains, sustainable development

## Introduction

With the intensification of global industrialization and agricultural practices, anthropogenic activities have exerted progressively greater pressure on groundwater systems, rendering nitrate contamination a pervasive and persistent challenge in water environmental management worldwide [1-7]. Owing to its high aqueous mobility, subsurface invisibility, and recalcitrance to conventional remediation, nitrate has long been a focal concern in hydrogeological and environmental research [8-10]. As early as the 1960s, the World Health Organization (WHO) established a health-based guideline value of 10 mg/L for nitrate-nitrogen ($NO_3^-$-N) in drinking water – primarily to safeguard infants against methemoglobinemia ("blue baby syndrome") – a benchmark that continues to serve as the foundational regulatory threshold for groundwater quality assessment across jurisdictions [6, 11-14]. Nevertheless, over the past five decades, a marked increase in synthetic nitrogen fertilizer application – compounded by diffuse emissions from intensive livestock operations and untreated or inadequately treated domestic wastewater – has facilitated widespread nitrogen loading into aquifers via leaching and infiltration. Consequently, $NO_3^-$-N concentrations frequently exceed the WHO threshold in key agricultural zones and urbanized catchments, underscoring critical gaps in current groundwater nitrogen pollution mitigation strategies [15-20]. Representative cases illustrate this trend across heterogeneous hydrogeological settings: in China's Miyun Reservoir watershed, synergistic inputs from agricultural runoff and domestic effluents generate pronounced spatial heterogeneity in nitrate distribution across surface–groundwater interfaces, thereby compromising regional drinking water security [21]; in the Woodville Karst Plain (USA), conduit-dominated flow pathways have enabled extensive nitrate plume propagation, perturbing long-term biogeochemical equilibrium within the aquifer [22]; and in the Sundarbans coastal aquifer system (India), the co-occurrence of intensive agriculture and seawater intrusion has elevated nitrate levels to hazardous concentrations, posing acute public health risks for communities reliant on groundwater for potable supply [23]. The overarching difficulty in addressing such geographically widespread and contextually variable contamination lies fundamentally in the inherent multiplicity and complexity of nitrate sources in groundwater systems. Major nitrogen inputs – including synthetic chemical fertilizers (CF), organic amendments (e.g., manure and sewage, MS), atmospheric nitrogen deposition (NAD), and native soil nitrogen (SN) – exhibit overlapping geochemical signatures and dynamic interplay, severely constraining source discrimination accuracy [24-28]. Early investigations predominantly employed conventional water chemistry approaches, inferring nitrate origins through temporal and spatial variations in dissolved $NO_3^-$, $NO_2^-$ and $NO_4^+$ concentrations at discrete discharge points. Yet these methods are highly susceptible to confounding effects from hydrological mixing, redox transformations, and microbial nitrogen cycling, limiting their diagnostic resolution in heterogeneous aquifer media [29, 30]. In contrast, advances in stable isotope geochemistry have established dual-isotope ($\delta^{15}N$–$\delta^{18}O$) analysis of nitrate as a robust and mechanistically grounded methodology for source apportionment and process tracing. Fundamentally, nitrate derived from distinct anthropogenic and natural reservoirs carries characteristic isotopic fingerprints: $\delta^{15}N$ reflects the extent and pathway of nitrogen transformation (e.g., nitrification, volatilization), whereas $\delta^{18}O$ encodes information on oxygen source (e.g., atmospheric $O_2$ vs. ambient water) and post-depositional processes (e.g., denitrification), collectively enabling discrimination among major input sources and quantification of in situ attenuation [11].

Initially, source identification relied almost exclusively on $\delta^{15}N$ alone [31-33]. However, accumulating empirical evidence reveals two principal limitations: (i) substantial overlap in baseline $\delta^{15}N$ ranges across common nitrate sources, and (ii) isotopic fractionation during denitrification – which preferentially removes $^{14}N$ and $^{16}O$ – distorts original source signals and introduces ambiguity in interpretation [34]. To address these constraints, the scientific community has increasingly adopted a coupled $\delta^{15}N$–$\delta^{18}O$ framework. This approach leverages the complementary sensitivity of the two isotopes: while $\delta^{15}N$ shifts primarily reflect nitrogen-source identity and transformation history, $\delta^{18}O$ provides independent constraints on reaction pathways and residence time. Cross-plotting $\delta^{15}N$ versus $\delta^{18}O$ values not only improves source resolution but also permits semi-quantitative estimation of denitrification extent – thereby enhancing both the precision of source attribution and the interpretability of biogeochemical dynamics in contaminated aquifers [2, 35-39].

Based on previous research findings, the nitrate concentration in some water bodies in the study area is relatively high (11.19 mg/L), posing risks to human health and crop growth. This study employs scientific methods to identify pollutant sources and provides recommendations for controlling pollutant

emissions, thereby effectively reducing pollution levels. A comprehensive sampling strategy was employed at multiple sites along the Han River and its tributaries, encompassing both upstream and downstream areas and spanning various time periods. These samples were then analyzed using stable isotope techniques, in conjunction with an assessment of local contextual factors, to infer the distribution patterns and sources of nitrate pollution.

## Materials and Methods

### Study Area

The upper reaches of the Han River serve not only as a crucial water source for the Middle Route of China's South-to-North Water Diversion Project but also as a water intake point for the "Yin-Han-Ji-Wei" Project in Shaanxi Province [40-42]. The study area is located at the junction of Chenggu County and Yang County in Hanzhong City, Shaanxi Province. It encompasses the Han River and its tributary, the Xushui River, as well as high floodplains ($I_0$), first to third terrace levels ($I_1$–$I_3$), and low mountains composed of Qingbaikou System metamorphic rocks (Fig. 1). Due to geological structures, the Qinling Mountains in the north and the Daba Mountains in the south confine the middle Han River valley. The overall topography is higher in the west and lower in the east, causing regional surface and subsurface flow to converge from the mountainous areas on both sides toward the central valley, thereby forming the Han River, which flows eastward into the Yangtze River. Consequently, the diffusion direction of pollutants in the water body aligns with the direction of water flow. The surrounding region is agriculturally prosperous, with crops such as rice, maize, wheat, and rapeseed cultivated in the basin, and tea and citrus fruits grown in the low mountainous regions.

The groundwater chemistry in the Hanzhong Basin is predominantly of the $HCO_3$–Ca type, primarily controlled by the weathering of carbonate and silicate rocks [43], with relatively minor influences from anthropogenic activities and cation exchange adsorption. The aquifers in the study area consist mainly of two types: unconfined groundwater and confined groundwater.

Unconfined aquifer: Thickness ranges from 55 to 74 m, with a burial depth of 3 to 20 m. Recharge sources include river infiltration, irrigation return flow, and precipitation infiltration. Confined aquifer: Thickness ranges from 34 to 46 m, with a water table depth

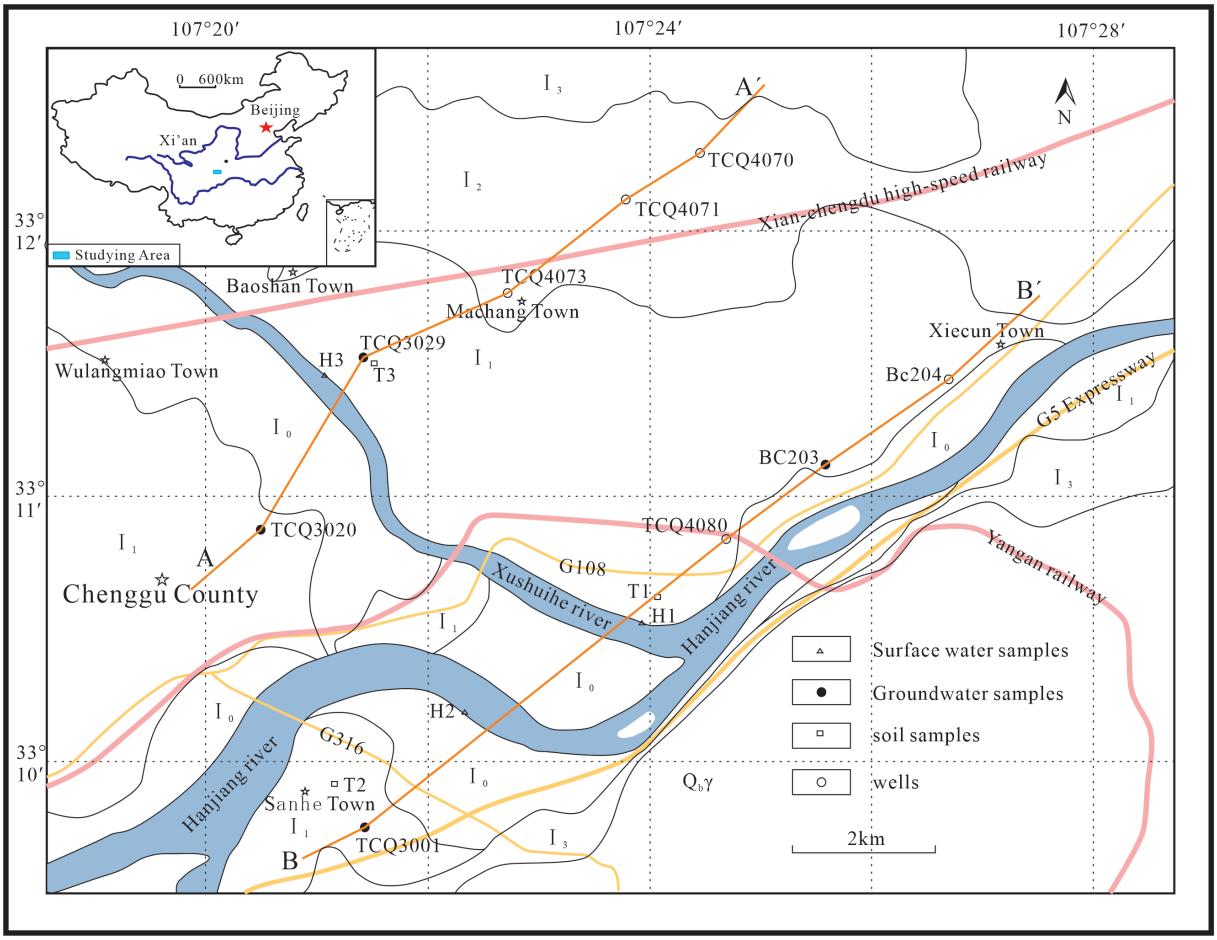



Fig. 1. Geological map of the study area and sampling sites.

of 6 to 35 m. Recharge occurs mainly through lateral runoff and leakage from the unconfined aquifer.

The study area is located at the junction of Chenggu County and Yang County in Hanzhong City, Shaanxi Province, with geographical coordinates ranging from 107°18′ to 107°30′E and 33°09′ to 33°13′N. This region features a comprehensive transportation network, including the G5 Expressway, G108 National Highway, Xi'an–Chengdu High-speed Railway, and Yang'an Railway. The Han River, oriented east–west, and the Xushui River – which joins the Han River from the northwest to the southeast – are accompanied by a network of minor tributaries and irrigation canals, contributing to the abundance of water resources in the area.

## Sample Layout and Sampling

Building upon previous water quality assessments, this study focuses on regions with substandard groundwater quality, classified as Categories III–IV. The primary research activities involve the establishment of two nitrogen-monitoring profiles and nine monitoring wells along the vertical direction of the groundwater flow field (Fig. 1), encompassing an area of approximately 100 $km^2$. Profile AA′ extends from the northeast corner of Chenggu County, crossing the Xushui River, to Liujiazhai Village in Yang County's Yuangong Town, while Profile BB′ stretches from Longwangmiao Village in Sanhe Town, Chenggu County, parallel to the Hanjiang River, to Zhiguo Village in Xiecun Town, Yang County. The nine monitoring wells are evenly distributed along the two profiles in a "four in the north, five in the south" pattern, effectively covering the first and second terrace levels and floodplains. The study employs groundwater flow field monitoring, comprehensive water quality analysis, and isotopic analysis to investigate the distribution, migration, and transformation patterns of nitrogen in groundwater, as well as to identify the sources of nitrate pollution. Additionally, soil profiles are analyzed to elucidate vertical variation patterns – revealing concentration changes with depth – and thereby provide a basis for formulating rational and effective pollution control strategies.

Sampling operations were conducted in two phases: the initial phase on April 8, 2021 (corresponding to the normal water level) and the subsequent phase on August 24, 2021 (during the high-water level period). The comprehensive sampling strategy incorporated three categories of specimens: water quality samples, soil elemental analysis samples, and isotopic analysis samples, totaling 35 distinct samples. A total of 14 water quality samples were collected (including 8 groundwater samples and 6 surface water samples); 11 isotopic samples were collected during the normal water level period (including 4 groundwater samples, 3 surface water samples, and 3 soil samples); and 3 sets of soil elemental analysis samples (10 samples per set) were collected during the high-water level period. The sampling locations were primarily situated on the floodplains and first terrace levels along the banks of the Han River and its tributary, the Xushui River.

The sample collection process is as follows: For surface water sampling, rinse the sample bottle three times with river water, then fill it with the water sample, seal it securely, and label it clearly; for groundwater sampling, pump water from the monitoring well for approximately 3 min to purge stagnant water, then rinse the sample bottle three times with well water (after discarding the initial surface water), fill it with the water sample, seal it securely, and label it clearly; for soil sampling, excavate to a depth of approximately 15 cm to remove the surface humic layer, then use a wooden shovel to collect a sufficient amount of soil, place it in a sample bag, and record the sample number. All samples were stored in a cool, dark place and transported to the testing laboratory the following day.

## Methods

The analytical scope encompassed comprehensive water quality analysis (including $HCO_3^-$), $\delta^{18}O$ and $\delta^{15}N$ isotope analysis, and soil elemental analysis. Concurrently, the groundwater level in each monitoring well was measured on-site biweekly.

Water quality analysis was conducted at the laboratory of Shaanxi Nuclear Industry Group Comprehensive Analysis and Testing Co., Ltd. The determination of major cations ($K^+$, $Na^+$, $Ca^{2+}$ and $Mg^{2+}$) was performed using an iCAP 6300 inductively coupled plasma optical emission spectrometer; anions ($Cl^-$, $NO_3^-$, $NO_2^-$ and $SO_4^{2-}$) and $NH_4^+$ were analyzed using an ICS-1100 ion chromatograph. The measurement error for cations and anions was less than 0.16%. $CO_3^{2-}$ and $HCO_3^-$ were measured by acidimetric titration using a 25 mL burette. Total dissolved solids (TDS) were determined by the oven-drying method with a BSA224S-CW electronic balance. pH was measured using a pHS-3C pH meter.

$\delta^{15}N$ values of water samples were measured at the Beijing Research Institute of Uranium Geology using a MAT-253 gas-source isotope ratio mass spectrometer, with a precision of ±2‰. $\delta^{18}O$ values were determined at the Xi'an Center of the China Geological Survey using an LGR liquid water isotope analyzer, with a measurement precision of ±2‰.

Soil sample analyses were conducted in accordance with established national standards. Total nitrogen, ammonium nitrogen, and nitrate nitrogen were determined following LY/T 1228–2015, whereas organic matter content was quantified according to NY/T 1121.6-2016. The Kjeldahl method was employed for total nitrogen analysis, achieving a precision of ±0.5 g/kg. For ammonium and nitrate nitrogen, a UV-2600 ultraviolet-visible spectrophotometer was used, with a detection limit of 0.2 mg/kg. Organic

matter was quantified via acidimetric titration, ensuring a precision of ±0.5 g/kg.

## Results

### Water Quality Assessment

According to the "Surface Water Environmental Quality Standard" (GB 3838–2002) and the "Groundwater Quality Standard" (GB/T 14848–2017), water quality is classified into five categories, with Class I representing the highest quality and Class V the lowest. Water quality below Class III is deemed unsuitable for potable use. The 2021 water quality assessment results for the study area are presented in Table 1:

Surface water conforms to Class I criteria, reflecting excellent quality. Groundwater $NO_3^-$–N concentrations ranged from 3.18 to 10.32 mg/L during the normal-flow period and from 2.6 to 8.4 mg/L during the high-flow period. These values generally meet Class II and Class III requirements; however, $NO_3^-$–N concentrations at several monitoring wells exceeded the WHO guideline value of 10 mg/L for drinking water.

### Spatial Distribution of Nitrate

#### *Spatial Distribution of Nitrate in Water*

Based on the multi-period groundwater level data from the nine wells, a groundwater flow direction map of the study area was delineated (Fig. 2). The map illustrates that near the surface runoff, groundwater flows downstream along the Han River and Xushui River from the upper reaches. In the northeastern part, away from the rivers, groundwater flows southeastward. Consequently, the groundwater flow direction is from northwest to southeast, aligning fundamentally with the course of the Han River and its tributary, the Xushui River.

Through the comparison of the data presented in Fig. 2 and Table 1, several conclusions can be drawn:

1. The predominant nitrate in surface water is nitrate nitrogen.

2. The concentration of nitrate nitrogen in surface water exhibits a decreasing trend, with H3>H2>H1, suggesting a gradual reduction in nitrate content from the upstream to the downstream regions.

3. The direction of nitrate content reduction aligns with the groundwater flow direction, implying that nitrate pollutants may originate from upstream areas.

4. Tributary rivers could potentially be the primary source of pollution.

5. As water flows downstream, pollutants tend to dissipate naturally.

In summary, it can be inferred that nitrate pollution in surface water is a process correlated with the direction of water flow, with the primary pollution source located in the upstream tributary, the Xushui River. As water migrates downstream, pollutant concentrations gradually decrease, which may be attributed to natural biochemical processes or dilution effects.

In groundwater, only nitrate nitrogen was detected as a nitrate pollutant. The results are discussed separately for periods of normal and high water levels. During the normal water level period, the nitrate nitrogen

Table 1. Analytical results of nitrogen species in the monitoring section.

| Test items | Period | BC203 | TCQ3001 | TCQ3020 | TCQ3029 | H1 | H2 | H3 |
|---|---|---|---|---|---|---|---|---|
| $NH_4^+$–N | Normal water level | ND | ND | ND | ND | 0.08 | 0.1 | 0.09 |
| $NO_3^-$–N | | 6.64 | 3.18 | 10.32 | 5.35 | 1.31 | 1.43 | 1.79 |
| $NO_2^-$–N | | ND | ND | ND | ND | 0.05 | 0.14 | 0.01 |
| $Ba^{2+}$ | | 59.5 | 108 | 57.4 | 33.0 | 23.8 | 31.6 | 22.2 |
| pH | | 8.39 | 8.50 | 8.23 | 8.33 | 8.68 | 8.54 | 8.50 |
| $NO_3^-$ | | 29.4 | 14.1 | 45.7 | 23.7 | 5.79 | 6.35 | 7.92 |
| $^{15}N$ | | 9.2 | 14.6 | 14.2 | 7.2 | 10.8 | 6.7 | 8.8 |
| $^{18}O$ | | -7.39 | -7.56 | -7.82 | -8.31 | -9.88 | -8.96 | -9.81 |
| $NH_4^+$–N | High water level | ND | ND | ND | ND | 0.068 | 0.075 | 0.075 |
| $NO_3^-$–N | | 4.3 | 2.6 | 8.0 | 8.4 | 0.7 | 1.0 | 1.3 |
| $NO_2^-$–N | | ND | ND | ND | ND | 0.052 | 0.043 | 0.049 |
| $Ba^{2+}$ | | 56.5 | 117 | 54.0 | 37.5 | 29.9 | 62.6 | 38.6 |
| pH | | 7.24 | 7.22 | 7.02 | 7.16 | 7.40 | 7.47 | 7.65 |

Notes: ND indicates not detected; the unit of $Ba^{2+}$ is μg/L; $^{15}N$ and $^{18}O$ are expressed in ‰; pH is dimensionless and all other measurements are mg/L.

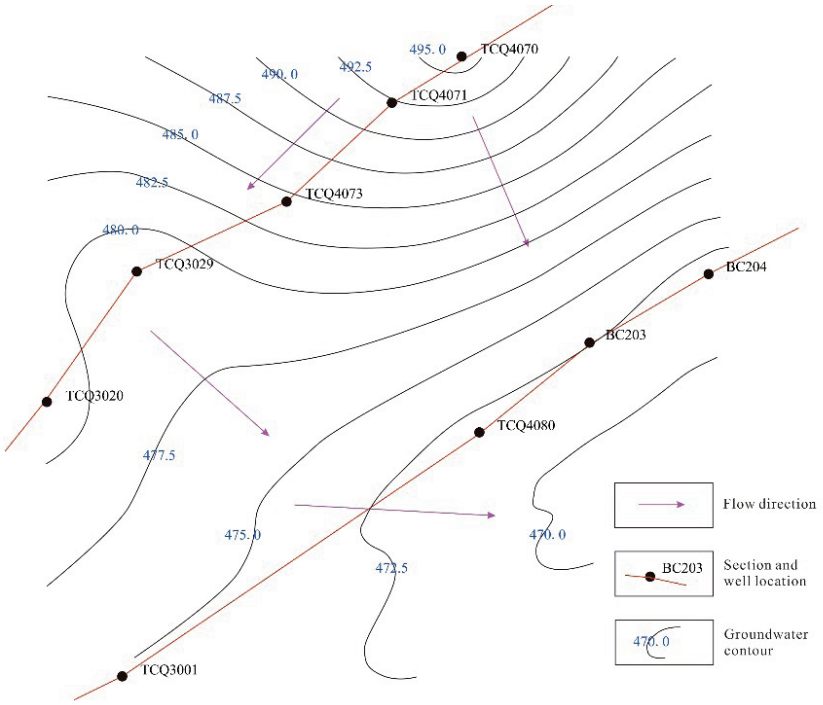



Fig. 2. Groundwater flow in the nitrogen monitoring section.

concentrations were ranked as TCQ3020>BC203 >TCQ3029>TCQ3001, indicating a downstream decrease in nitrate content from the upstream areas. This reduction aligns with the groundwater flow direction, suggesting that nitrate pollutants originate from upstream sources, with the main pollution source located at the Xushui River tributary. However, a secondary pollution source was observed near the downstream monitoring well BC203. Pollutants naturally attenuate as they flow downstream. During the high water level period, the nitrate nitrogen concentrations were ranked as TCQ3029>TCQ3020>BC203>TCQ3001, reflecting a consistent trend in nitrate content changes between groundwater and surface water.

Therefore, during normal and high water levels, the trend of nitrate pollution in surface water and groundwater is consistent. The differences are that during normal water levels, the overall pollutant content is higher and that there are additional pollution sources near the downstream monitoring well BC203.

### *Spatial Distribution of Nitrate Pollution in Soil*

Soil is the cornerstone of agricultural production, serving as the primary medium for crop growth, with the majority of plant roots developing within it. Additionally, soil acts as a conduit for the transport of nutrients, including water and trace minerals, which are absorbed by plant roots through the soil. Finally, soil itself is a source of essential nutrients.

The data presented in Table 2 indicate a consistent pattern in the distribution of nitrate concentrations across the three sampling points. Notably, the highest nitrate levels were observed at Point 2, followed by Point 3, with the lowest levels at Point 1. This distribution aligns with the direction of groundwater flow, suggesting that the migration and distribution of nitrates are influenced by groundwater movement.

Specifically, the total nitrogen content is highest in the topsoil and decreases gradually with depth, indicating that the surface soil is most severely affected by agricultural irrigation. Although water-soluble ammonium and nitrate nitrogen also show higher concentrations in the top layer and generally decrease with depth, their concentrations suddenly increase and surpass those in the surface layer at approximately 1 meter below ground, suggesting that the lower soil may be influenced by nitrate-containing groundwater, leading to a sudden increase in nitrogen content. Similarly, the organic matter content increases around 1 meter below ground but does not exceed that in the surface layer.

## Discussion

### Determination of Nitrification and Denitrification

Due to the refractory nature of nitrogen, various factors can influence the nitrogen isotope composition in groundwater. This composition is determined not only by the isotopic characteristics of the nitrate pollution source but also by the physical, chemical, and biochemical processes that nitrate undergoes upon entering the groundwater. These processes can alter the original isotopic composition of nitrate in the groundwater. Consequently, it is essential to assess

these factors before identifying the sources of nitrate pollution.

In the water-soil environment, processes such as nitrification, denitrification, and ammonia volatilization can cause nitrogen isotope fractionation, leading to changes in the isotopic composition of nitrate in groundwater. Among these, ammonia volatilization is a physicochemical process significantly influenced by pH. Generally, the critical pH value for the conversion of $NH_4^+$ to $NH_3$ in aqueous solutions is 9.3 [44]. An increase in pH favors ammonia volatilization, whereas a decrease results in nitrogen predominantly existing in the ionic form $NH_4^+$. As indicated in Table 1, the pH values of the samples in this study are all below 9.3; therefore, ammonia volatilization is not considered a significant factor.

Let us discuss the processes of denitrification and nitrification in detail.

*Determination of Denitrification*

Denitrification typically occurs under anaerobic conditions in the presence of organic matter. It is a process whereby denitrifying bacteria convert $NO_3^-$ into $N_2$, represented by Equation (1):

$$4NO_3^- + 5C + 2H_2O \rightarrow 2N_2 + 4HCO_3^- + CO_2 \quad (1)$$

As shown in Equation (1), during the reaction, the concentrations of reactants and products change. Initially, this is manifested by an increase in the $\delta^{15}N$ value of the residual nitrate as the $NO_3^-$–N concentration decreases [35, 36]. Additionally, there is synchronous enrichment of $\delta^{15}N$ and $\delta^{18}O$, with the $\delta^{15}N/\delta^{18}O$ ratio approximately equal to 2:1 [12, 17, 45-48]. These two indicators can corroborate one another, thereby enabling more effective identification of denitrification.

Based on the above information, Fig. 3 illustrates a linear positive correlation between $\delta^{15}N$ values and nitrate ($NO_3^-$) concentrations, indicating that an increase in $NO_3^-$ concentration corresponds to an increase in $\delta^{15}N$ values. This relationship provides evidence that denitrification is not occurring within the aquifer of the study area. Furthermore, the $\delta^{15}N/\delta^{18}O$ ratio depicted in Fig. 4 deviates from the ~2:1 ratio characteristic of typical denitrification processes, suggesting that substantial denitrification is unlikely in the study region. Consequently, the $\delta^{15}N$ and $\delta^{18}O$ signature values of nitrate in groundwater can be used to identify the sources of nitrate contamination.

*Determination of Nitrification*

Nitrification is a two-step aerobic process in which ammonium ($NH4^+$) is oxidized to nitrate ($NO_3^-$). This involves the transformation of nitrogen from its reduced form ($NH_4^+$) to an intermediate oxidized form ($NO_2^-$) and then to a fully oxidized state ($NO_3^-$). The oxidation state of nitrogen changes from –3 in $NH_4^+$ to +5 in $NO_3^-$. This transformation is represented by Equation (2):

$$NH_4^+ + 2O_2 \rightarrow NO_3^- + 4H^+ + H_2O \quad (2)$$

Table 2. Analytical results of soil vertical profiles.

| No. | Bottom depth (m) | Lithology | Total nitrogen (g/kg) | Ammonium nitrogen (mg/kg) | Nitrate nitrogen (mg/kg) | Organic matter (g/kg) |
|---|---|---|---|---|---|---|
| T1-1 | 0.3 | Gray silt interbedded with fine sand | 0.48 | 14.4 | 1.65 | 11.5 |
| T1-2 | 0.5 | Gray silt with fine sand | 0.55 | 4.68 | 1.10 | 2.78 |
| T1-3 | 0.7 | Yellow-brown silty clay | 0.64 | 3.57 | 0.11 | 2.92 |
| T1-4 | 0.9 | Yellow-brown silty clay | 0.50 | 7.13 | 0.13 | 1.94 |
| T1-5 | 1.0 | Yellow-brown silty clay | 0.42 | 3.18 | 3.46 | 4.56 |
| T2-1 | 0.2 | Grayish-white soil interbedded with medium to coarse sand | 1.20 | 11.6 | 31.1 | 15.2 |
| T2-2 | 0.7 | Yellow-brown silty clay interbedded with fine sand | 0.32 | 16.1 | 11.7 | 0.96 |
| T2-3 | 1 | Grayish-green silt interbedded with coarse sand | 0.29 | 38.8 | 0.34 | 1.92 |
| T3-1 | 0.4 | Gray silty clay with minor layers of fine sand | 1.32 | 10.1 | 2.58 | 9.08 |
| T3-2 | 0.7 | Yellow-brown silty clay | 0.78 | 7.54 | 0.48 | 6.93 |
| T3-3 | 1 | Brownish-yellow silty clay with minor gravel | 0.65 | 12.4 | 4.33 | 7.05 |

Note: The sampling interval thickness is 10 cm.

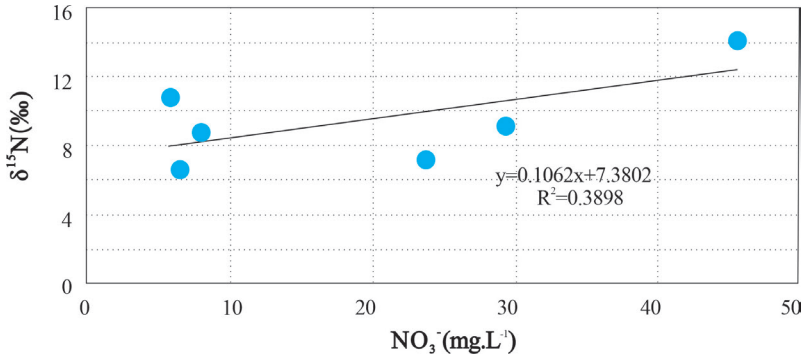



Fig. 3. Relationship between $\delta^{15}N$ value and $NO_3^-$ concentration.

As shown in Equation (2), during nitrification, the production of $NO_3^-$ increases, and its $\delta^{18}O$ value may decrease continuously with rising $NO_3^-$ concentration.

During nitrification, the oxygen isotopes ($\delta^{18}O$) in the newly formed nitrate ($NO_3^-$) become lighter relative to those in the reactants – particularly the oxygen in water molecules ($H_2O$) – due to oxygen isotope fractionation. This occurs because ammonia-oxidizing and nitrite-oxidizing bacteria preferentially incorporate the lighter oxygen isotope ($^{16}O$) during oxidation to form $NO_3^-$, resulting in enrichment of the heavier isotope ($^{18}O$) in the residual reactants.

Research indicates that nitrification yields nitrate $\delta^{18}O$ values ranging from –10‰ to –7‰ [12, 17, 18, 48]. This range serves as an isotopic fingerprint of nitrification. Moreover, the gradual decrease in $\delta^{18}O$ values – from soil (–4.41‰ to –3.98‰) to groundwater (–8.32‰ to –7.40‰) and then to surface water (–9.89‰ to –8.96‰) – reflects the occurrence and environmental impact of nitrification across different media. In contrast, $\delta^{15}N$ values exhibit minimal change during nitrification, as nitrogen isotope fractionation is far less pronounced than oxygen isotope fractionation in this process. This implies that while nitrification strongly affects $\delta^{18}O$ values of nitrate, it induces negligible shifts in $^{\delta 15}N$ values.

## Source of Nitrate Contamination

The distinct isotopic compositions of nitrogen and oxygen in nitrates from various sources enable their differentiation. Nitrate originating from soil organic nitrogen exhibits $^{\delta 15}N$ values between 4‰ and 9‰. In contrast, nitrate derived from inorganic fertilizers has $^{\delta 15}N$ values ranging from –4‰ to 4‰. Nitrate from sewage or fecal matter displays $^{\delta 15}N$ values from 9‰

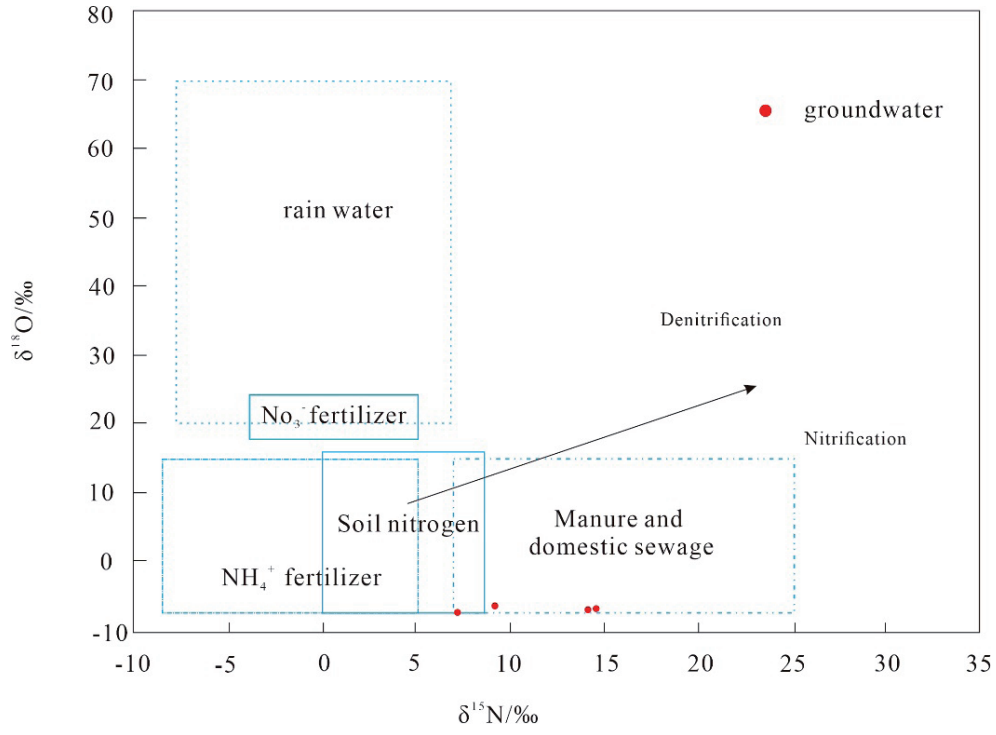



Fig. 4. Ranges of $\delta^{15}N$ and $\delta^{18}O$ values of nitrate nitrogen from different sources.

to 20‰ [18], and nitrate from animal manure falls within the range of 8.8‰ to 9‰ [49, 50]. Atmospheric deposition yields nitrate with $\delta^{18}O$ values ranging from 18‰ to 70‰ [47, 48], whereas fertilizer-derived nitrate typically exhibits $\delta^{18}O$ values of 22‰±3‰ [26, 36, 50, 51]. Microbial nitrification produces nitrate with $\delta^{18}O$ values between –10‰ and +10‰ [36, 49, 52]. A diagnostic diagram (Fig. 4, [16]) based on these isotopic signatures has been constructed for rapid source identification.

In the absence of denitrification, the study area's analytical results were plotted onto a dual-isotope ($\delta^{15}N$ vs. $\delta^{18}O$) diagram representing typical isotopic ranges for different nitrogen sources (Fig. 4). The data points fall within the overlapping ranges associated with soil nitrogen, animal manure, and domestic wastewater. Further interpretation was conducted in conjunction with the local environmental and land-use conditions.

The study area is located at the confluence of the Xushui River and the Han River in the Hanzhong Basin. It is characterized by flat terrain and an extensive river network, and lies in a rural region where agriculture is the dominant economic activity – supplemented by poultry farming and a few pig farms – with no industrial operations present. Domestic sewage is commonly discharged directly into ditches and rivers, which subsequently serve as irrigation sources for farmland. Additionally, the widespread practice of applying animal manure as crop fertilizer, along with the construction of septic tanks adjacent to vegetable fields in some villages, contributes to the potential nitrate contamination of groundwater. Moreover, the presence of a continuous soil layer above the aquifer in this region makes soil organic nitrogen a plausible source of nitrate pollution in groundwater [3, 12].

Consequently, the primary sources of nitrate contamination in the groundwater of the study area are identified as MS and SN.

### Sustainable Development Strategy

Agricultural production frequently leads to nitrate accumulation in soil and groundwater systems. This accumulation significantly impedes the sustainable development of agricultural regions and may trigger multiple adverse effects. From an environmental perspective, elevated nitrate concentrations can contaminate water bodies and cause eutrophication, disrupting aquatic ecosystems and potentially inducing harmful algal blooms. These phenomena degrade water quality and pose serious threats to biodiversity. Regarding public health, consumption of water with high nitrate concentrations is hazardous – potentially increasing healthcare expenditures and diminishing the overall quality of life for affected populations. Although nitrates are essential for plant nutrition, excessive levels can cause soil nutrient imbalances, reduce crop yields, and thereby compromise food security. Furthermore, the economic costs of managing nitrate pollution in soil and water systems are substantial, including expenses related to treating contaminated water supplies and restoring degraded ecosystems.

Understanding the spatial distribution and origin of nitrate contamination is critical for developing effective management and mitigation strategies. Such knowledge enables policymakers and agricultural stakeholders to implement targeted interventions – such as promoting sustainable farming practices, upgrading waste management infrastructure, and routinely monitoring nitrate concentrations in groundwater and soil. Proactively addressing these issues safeguards public health, ensures food security, and supports the long-term sustainability of agricultural systems.

Addressing these challenges is paramount to fostering sustainable agricultural development in the study area. Priority efforts should focus on mitigating nitrate pollution from its principal sources. Research indicates that incorporating straw into the soil significantly enhances crop yields and nitrogen uptake efficiency, thereby reducing nitrate leaching from soil and lowering its concentration in groundwater [12, 29, 30, 43]. Additionally, improved management of animal manure and domestic wastewater is essential. This includes accelerating the renovation of rural dry toilets, strengthening discharge controls, and enhancing wastewater treatment capacity. Finally, advancing precision agriculture is crucial: it involves increasing the use of organic fertilizers and improving the application efficiency of chemical fertilizers and urea, thereby reducing total application rates.

Researchers in agricultural pollution areas have measured the concentrations of cholestanol (5α) and coprostanol (5β), using the sterol ratio (5β/(5β+5α)) to determine the origins of pollutants from animal feces, providing new insights for pollution source control [13, 14, 17, 18, 53]. Given the complex sources of nitrate pollutants in groundwater and the variability of nitrogen and oxygen isotopic values over time and space, further monitoring and tracking research are required [1, 4, 54]. Moreover, the implementation of effective policies and regulations, raising public awareness, and investing in research and development of sustainable agricultural practices are key steps to mitigating the impacts of nitrate pollution.

## Conclusions

This study investigates a representative watershed at the Chenggu-Yangxian county boundary in the upper Han River basin, situated on the southern piedmont of the Qinling Mountains. Using multi-medium coordinated sampling during both baseflow and high-flow periods, we conducted a systematic analysis of nitrate distribution, migration behavior, and source apportionment in groundwater. The principal findings are summarized as follows:

(1) Overall water quality in the study area is excellent: surface water complies with Class I standards, while groundwater is predominantly classified as Class II-III, with isolated instances of anomalous nitrate-nitrogen enrichment. Nitrate spatial distribution exhibits strong concordance with the northwest-to-southeast groundwater flow direction. The primary contamination sources are located in the upstream Xushui River catchment. Nitrate concentrations during baseflow periods are markedly higher than during high-flow periods, and a pronounced downstream attenuation trend is observed along the flow path. A critical interface for localized nitrate accumulation occurs at approximately 1 m depth.

(2) Nitrogen transformation in the groundwater system is predominantly governed by nitrification, with no substantial evidence of denitrification or ammonia volatilization. Along the soil-groundwater-surface water continuum, $\delta^{18}O$ values of nitrate decrease progressively – a pattern fully consistent with isotopic fractionation associated with natural nitrification. This process significantly affects oxygen isotopic composition but exerts negligible influence on nitrogen isotopes, thereby establishing a robust isotopic basis for precise pollution source identification.

(3) Integrating stable isotope fingerprinting with regional land-use data, we attribute the dominant nitrate sources in groundwater to indigenous soil nitrogen, livestock manure, and domestic wastewater. In light of the region's agriculture-based economy characterized by dispersed small-scale livestock operations, we propose a spatially differentiated management strategy comprising straw incorporation to enhance nitrogen use efficiency, standardized management of rural sewage and manure, and adoption of precision fertilization practices. These interventions provide technically grounded, source-targeted support for advancing green and sustainable agriculture and safeguarding drinking water source quality.

## Data Availability Statement

The data described in the manuscript can be obtained from the corresponding author upon reasonable request.

## Acknowledgments

The authors sincerely thank Jun Zhang for his valuable assistance with isotope analysis.

## AI Usage Disclosure Statement

Artificial Intelligence Tool Usage Statement: During manuscript preparation, only Youdao Translation (2026 official PC version) was employed to support the initial translation of Chinese academic content into English. All translated text underwent rigorous, sentence-by-sentence review, revision, and validation by the first author and the corresponding author – both of whom possess disciplinary expertise and native-level academic English proficiency. All substantive research activities – including study design, data collection, conceptual reasoning, manuscript drafting, and interpretation of results – were conducted independently by the authors. All original research data were generated and analyzed without AI assistance. AI tools contributed exclusively to linguistic support and played no role in the conception, execution, or interpretation of the scientific work.

## Funding

This work was jointly supported by the Geological Survey Projects of the China Geological Survey (Grant Nos. DD202607102405, DD202607102104, DD20208068) and the Natural Science Basic Research Program of Shaanxi Province (Grant No. 2025JC-YBQN-424).

## Conflict of Interest

The authors declare no conflict of interest.

## References

1. BOURAOUI F., UDIAS A., VIGIAK O., GRIZZETTI B. 30 years of Nitrates Directive in a changing climate: Environmental and policy impacts on nutrient pollution of French rivers. Journal of Hydrology: Regional Studies, **65**, 103445, **2026**.
2. ALASSANE ZAKARI A., KPEGLI K.A.R., GNAZOU D.-T.M., ALASSANE A., GUIDAH CHABI B., LAWSON F.M.A., YALO N., MAMA D., BOUKARI M. Groundwater hydrochemistry and identification of nitrate pollution sources in the Ouémé Delta (Southern-Benin) using dual isotopes ($^{15}N–NO_3$ and $^{18}O–NO_3$) and a Bayesian isotope mixing model. Case Studies in Chemical and Environmental Engineering, **13**, 101303, **2026**.
3. TONG H., GAO R., YUE C., XIE L., DUAN L., ZHU Y., WANG G. Hydrochemical evolution and nitrate sources, migration, and transformation in surface water and groundwater of a typical tributary of the Yellow River. Journal of Environmental Management, **390**, 126218, **2025**.
4. BORAH P., BORAH G., MALAKAR A. Mitigating nitrate contamination in groundwater: A comprehensive review of in-situ approaches. Groundwater for Sustainable Development, **28**, 101406, **2025**.
5. LI P., WU J., HE X., WANG Y., REN X., LI L. Groundwater Nitrate Pollution and Health Risks Under Land Use Changes. Springer Nature Switzerland, Cham, **2026**.
6. SOULA R., CHEBIL A., CETIN M., MAJDOUB R. Spatial analysis and geostatistical characterization of nitrate pollution in Mahdia's shallow aquifers. Environmental Science and Pollution Research, **32** (27), 16380, **2025**.

7. NAKAGAWA K., AMANO H., SHINKAI F., WAKASA A., BERNDTSSON R. Integrated approach to investigate groundwater nitrate nitrogen pollution and remediation simulation in Shimabara Peninsula, Nagasaki, Japan. Environmental Earth Sciences, **84** (10), 256, **2025**.
8. BIDDAU R., DORE E., DA PELO S., LORRAI M., BOTTI P., TESTA M., CIDU R. Geochemistry, stable isotopes and statistic tools to estimate threshold and source of nitrate in groundwater (Sardinia, Italy). Water Research, **232**, 119663, **2023**.
9. XUE Y., ZHANG Y., WANG H., ZHANG L., LI H. Seawater intrusion and nitrate pollution in coastal fishery areas: An integrated hydrogeological, hydrochemical, and isotopic approach. Marine Environmental Research, **213**, 107668, **2026**.
10. LIU Y., QIAN H., GAO Y., LI S., SHI X., CAO Z., LONG Q., HE Y., MA Y., WU P., SHEN Y. Identifying nitrate pollution of groundwater based on aquifer vulnerability and surface nitrogen loads in the Northern Foot of the Qinling Mountains, China. Journal of Hazardous Materials, **495**, 138939, **2025**.
11. CAO S., YANG G., ZHOU J., LIU J., LIU C., LI J., LI Y. Nitrate pollution sources and associated biogeochemical mechanisms in coastal groundwater affected by seawater intrusion using multiple isotopes and source apportionment models. Marine Pollution Bulletin, **232**, 120059, **2026**.
12. TIAN P., QIAN H., LI S., SHI X., LI K., LIU Y., GAO Y., CAO Z., WU P., MA Y. Distribution, source apportionment, and non-carcinogenic health risk assessment of nitrate pollution in surface and groundwater of the Yi River Basin, China. Journal of Hydrology: Regional Studies, **64**, 103237, **2026**.
13. HUANG S., GUO J., XIE Y., BIAN R., WANG N., QI W., LIU H. Distribution, sources, and potential health risks of fluoride, total iodine, and nitrate in rural drinking water sources of North and East China. Science of The Total Environment, **898**, 165561, **2023**.
14. SAN A., KHANT N.A., MOON J., KIM H. Groundwater nitrate pollution in Myanmar and policy implications for sustainable water management. Hydrogeology Journal, **34** (3), 749, **2026**.
15. ZHANG Q., XU P., QIAN H., WEI A., CAO K. Nitrate pollution mechanisms and health risk assessment of shallow groundwater in a millennium-cultivated region of China. Physics and Chemistry of the Earth, Parts A/B/C, **143**, 104363, **2026**.
16. WANG K., ZHAO W., GUO J., YANG L., LI S., DAI J. Spatiotemporal variations in groundwater nitrate and its sources regulated by external inputs and soil profile characteristics in an agricultural basin. Journal of Hazardous Materials, **500**, 140571, **2025**.
17. CHAI G., YANG F., LIAO H., JIA D., FENG W., HO C., LIU D., CHEN S., LIU J., YU H. Coupling of spectroscopy and nitrogen-oxygen isotopes unveils the mechanisms of dissolved organic matter and nitrate pollution in lakes within the agro-pastoral transition zone. Journal of Environmental Sciences, **168**, 371, **2026**.
18. CHEN Q., WANG C., CHEN A., CUI R., HU W., FU B., JIANG C., CHEN X., ZHANG D. Source apportionment and uncertainty assessment of nitrate and phosphate pollution in shallow groundwater in agricultural watersheds based on multi-isotope methods. Groundwater for Sustainable Development, **32**, 101561, **2026**.
19. WANG H., ISHII S. Bioremediation of agricultural nitrate pollution – challenges and opportunities. Water Research X, **29**, 100410, **2025**.
20. SI W., ZHOU H., XU J., XIE Z., ZHANG M., LIU G., WANG C. Water transformations and nitrate pollution sources in typical agricultural watershed of China during the Dry Season. Journal of Environmental Sciences, **169**, 137, **2026**.
21. CHEN R., WANG Y., YANG S., WANG Y., ZHI W. Source apportionment of nitrate pollution in the reservoir basins based on dual isotopes of nitrogen and oxygen. Journal of Contaminant Hydrology, **281**, 104980, **2026**.
22. XU Z., HU B.X., DAVIS H., CAO J. Simulating long term nitrate-N contamination processes in the Woodville Karst Plain using CFPv2 with UMT3D. Journal of Hydrology, **524**, 72, **2015**.
23. PAL S.C., BISWAS T., JAYDHAR A.K., RUIDAS D., SAHA A., CHOWDHURI I., MANDAL S., ISLAM A., ISLAM A.R.M.T., PANDE C.B., ALAM E., ISLAM M.K. Source identification and potential health risks from elevated groundwater nitrate contamination in Sundarbans coastal aquifers, India. Scientific Reports, **14** (1), 4153, **2024**.
24. LIU X., HAN Z., LI Q., WU P. Quantitative identification of nitrate pollution sources in karst water in carbonate basins combined with stable isotope tracer techniques. Ecohydrology & Hydrobiology, **25** (3), 573, **2025**.
25. MONDAL M., SEN S., MUKHERJEE A., DAS K. Lateral and vertical solute transport controlling groundwater pollution in the Sundarbans: Insights from nitrate concentration and stable isotopic signatures. Science of The Total Environment, **1048**, 182043, **2026**.
26. NING J., LI P., WU J., YUAN Z., XU F., ZHENG L. Source apportionment of groundwater nitrate pollution in irrigation districts along the Jing River, Guanzhong Basin: Insights from hydrochemistry, isotopes, and the MixSIAR model. Journal of Environmental Chemical Engineering, **13** (3), 116231, **2025**.
27. CHEN W., HU L., LI J., LIN X., YANG X. Spatiotemporal heterogeneity, source apportionment, and transformation-driven partitioned control of nitrate pollution in urban river network: Isotopic and Bayesian insights from the Liuxi-Baini River Basin. Journal of Environmental Chemical Engineering, **14** (2), 121552, **2026**.
28. ZHENG J., GUO X., CAI Y., LIU J., WANG D., GAO X., TAN B. Source apportionment and health risks of nitrate pollution in shallow groundwater in the agricultural Northern Xiaoxing‘ an Mountains region of China. Journal of Hydrology: Regional Studies, **59**, 102394, **2025**.
29. ZHANG Y., XIE Z., LIU W., HUANG J., CHEN S., ZHANG X., YANG C., LI J., KANG W., WANG Y. Source identification and health risk assessment of urban groundwater nitrate contamination in Chongqing, southwestern China. Journal of Hydrology: Regional Studies, **62**, 102792, **2025**.
30. UDESHANI C., YUE F.J., GONG Y.Q., LI S.L., CHANDRAJITH R. Sources and dynamics of nitrate in groundwater in a crystalline terrain of tropical Sri Lanka based on a dual isotope approach. Water Research, **282**, 123914, **2025**.
31. KOHL D.H., SHEARER G.B., COMMONER B. Fertilizer Nitrogen: Contribution to Nitrate in Surface Water in a Corn Belt Watershed. Science, **174** (4016), 1331, **1971**.
32. VOGEL J.C., TALMA A.S., HEATON T.H.E. Gaseous nitrogen as evidence for denitrification in groundwater. Journal of Hydrology, **50**, 191, **1981**.
33. MCMAHON P.B., BÖHLKE J.K. Denitrification and mixing in a stream – aquifer system: effects on nitrate

loading to surface water. Journal of Hydrology, **186** (1-4), 105, **1996**.
34. DENG Q., WU X., ZHANG W., LI C., ZHANG L., TENG Y., ZHANG Y., LI G. Characteristics and source analysis of nitrate pollution of karst groundwater in the Xiaoli area of the lower Yellow River Basin. Applied Water Science, **16** (7), 213, **2026**.
35. SAMBORSKA-GOIK K., WASSENAAR L.I. Reimagining the Kendall plot: using $\delta^{15}N$ and $\delta^{18}O$ of nitrate and advanced machine learning to improve N pollutant source classification. Isotopes in Environmental and Health Studies, **61** (3), 310, **2025**.
36. LONG R., TIAN F., CHEN J.H., ZHOU Y.B., LI X.F., LI Y.T., TANG H.W., CHEN H.G. Source apportionment of nitrate in the Pearl River Estuary using $\delta^{15}N$ and $\delta^{18}O$ values and isotope mixing model. Marine Pollution Bulletin, **191**, 114962, **2023**.
37. XU B., LIN Y., WU Y., WANG Y. Identifying sources and transformations of nitrate in different occurrence environments of carbonate rocks using a coupled isotopic approach ($\delta^{15}N$, $\delta^{18}O$, $^{87}Sr/^{86}Sr$) in karst groundwater system, North China. Science of The Total Environment, **912**, 169300, **2024**.
38. JI X., SHU L., LI J., ZHAO C., CHEN W., CHEN Z., SHANG X., DAHLGREN R. A., YANG Y., ZHANG M. Tracing nitrate sources and transformations using $\Delta^{17}O$, $\delta^{15}N$, and $\delta^{18}O$-$NO_3^-$ in a coastal plain river network of eastern China. Journal of Hydrology, **610**, 127829, **2022**.
39. MADRIGAL-SOLÍS H., VADILLO-PÉREZ I., JIMÉNEZ-GAVILÁN P., FONSECA-SÁNCHEZ A., QUESADA-HERNÁNDEZ L., CALDERÓN-SÁNCHEZ H., GÓMEZ-CRUZ A., MURILLO J.H., SALAZAR R.P. A multidisciplinary approach using hydrogeochemistry, δ15NNO3 isotopes, land use, and statistical tools in evaluating nitrate pollution sources and biochemical processes in Costa Rican volcanic aquifers. Science of The Total Environment, **951**, 174996, **2024**.
40. ZHANG H., LUO J., WU J., DONG H. Dynamic multiobjective two-stage fuzzy stochastic strategy for optimal water allocation in inter-basin water division under changing environment: A case study of Hanjiang-to-Weihe water division in Shaanxi Province, China. Journal of Cleaner Production, **452**, 142175, **2024**.
41. LAI Y., CHENG L., FU C., WU Y., WANG S., HOU Q., LIU P., ZHANG L. Ecohydrological characteristics of a typical small catchment in the Upper Han River Basin: Insights from field measurements and modelling. Journal of Hydrology: Regional Studies, **66**, 103558, **2026**.
42. JIANG X., WANG J., LIU X., CHEN S., YI L. Impact of landscape patterns on solute dynamics during hydrological events: A multiscale study in the upper Han River basin. Ecological Indicators, **176**, 113722, **2025**.
43. HAN C.H., WANG Z.R., TIAN H., NIU Q.S., LIU L., ZHU Y.L., DING L.C., ZHAO L.L., ZHAO H., ZHAO C., WANG F., LI X.B., GONG W.Q. Hydrochemical Characteristics and Genesis of Groundwater in the Hanzhong Basin. Northwestern Geology, **56** (4), 263, **2023** [In Chinese].
44. KOROM S.F. Natural denitrification in the saturated zone: A review. Water Resources Research, **28** (6), 1657, **1992**.
45. WANG S., CHEN J., ZHANG S., BAI Y., ZHANG X., CHEN D., HU J. Groundwater hydrochemical signatures, nitrate sources, and potential health risks in a typical karst catchment of North China using hydrochemistry and multiple stable isotopes. Environmental Geochemistry and Health, **46** (5), 173, **2024**.
46. YU L., ZHENG T., ZHENG X., HAO Y., YUAN R. Nitrate source apportionment in groundwater using Bayesian isotope mixing model based on nitrogen isotope fractionation. Science of The Total Environment, **718**, 137242, **2020**.
47. JIN Z., WANG J., CHEN J., ZHANG R., LI Y., YAOTING L., HE K. Identifying the sources of nitrate in a small watershed using $\delta^{15}N$-$\delta^{18}O$ isotopes of nitrate in the Kelan Reservoir, Guangxi, China. Agriculture, Ecosystems & Environment, **297**, 106936, **2020**.
48. KRUK M.K., MAYER B., NIGHTINGALE M., LACEBY J.P. Tracing nitrate sources with a combined isotope approach ($\delta^{15}N$-$NO_3$, $\delta^{18}O$-$NO_3$ and $\delta^{11}B$) in a large mixed-use watershed in southern Alberta, Canada. Science of The Total Environment, **703**, 135043, **2020**.
49. LORETTE G., SEBILO M., BUQUET D., LASTENNET R., DENIS A., PEYRAUBE N., CHARRIERE V., STUDER J.-C. Tracing sources and fate of nitrate in multilayered karstic hydrogeological catchments using natural stable isotopic composition ($\delta^{15}N$-$NO_3^-$ and $\delta^{18}O$-$NO_3^-$). Application to the Toulon karst system (Dordogne, France). Journal of Hydrology, **610**, 127972, **2022**.
50. LI Y., YANG Z., KANG F.X., LIU J.Y., SUN Y.W., HUANG J.B. Isotope analysis on the source of nitrate contamination to groundwater in the Dong'e hydrogeologic unit. Carsologica Sinica, **38** (1), 19, **2019**.
51. WANG S., LI H., KANG T., LI R.X., ZHANG C.Z. Resolving nitrate sources in rivers through dual isotope analysis of $\delta^{15}N$ and $\delta^{18}O$. Water, **17** (23), 3370, **2025**.
52. SUN X.B., GUO C.L., ZHANG J., SUN J.Q., CUI J., LIU M.H. Spatial-temporal difference between nitrate in groundwater and nitrogen in soil based on geostatistical analysis. Journal of Groundwater Science and Engineering, **11** (1), 37, **2023**.
53. NAKAGAWA K., AMANO H., PERSSON M., BERNDTSSON R. Spatiotemporal variation of nitrate concentrations in soil and groundwater of an intensely polluted agricultural area. Scientific Reports, **11** (1), 2598, **2021**.
54. RUMAN M., DĄBROWSKA D. Evaluation of Water Quality from the Zimny Sztok Spring (Southern Poland) – Preliminary Results. Sustainability, **16** (12), 4962, **2024**.